International Journal of Heat and Mass Transfer 52 (2009) 5167–5172

Contents lists available at ScienceDirect

International Journal of Heat and Mass Transfer

journal homepage: www.elsevier.com/locate/ijhmt

Formation and sublimation of ice structures over cylindrical collectors

Guillermo G. Aguirre Varela, Nesvit E. Castellano, Eldo E. Ávila *

Facultad de Matemática Astronomía y Física, Universidad Nacional de Córdoba, CONICET, Ciudad Universitaria, 5000 Córdoba, Argentina

ARTICLE INFO

Article history:
Received 10 October 2008
Received in revised form 14 April 2009
Available online 12 June 2009

Keywords:
Ice sublimation
Ice accretion
Lobe's structure
Ice morphology

ABSTRACT

A series of experiments were conducted for temperatures below 0 °C, air velocities of 5, 8 and 11 m s^{-1}, with the goal of studying the structural characteristics and sublimation of ice structures grown over cylindrical rotating collectors. The results show that the accreted ice presents structures similar to lobes. A connection between the surface characteristics of the accretion and the environmental conditions was established. It was also found that the size and lobe-number density of the ice accreted on the surface do not affect sublimation rate when the sublimation process occurs in free convection conditions.

1. Introduction

A cloud or fog consists of small water droplets or ice crystals. Even if the temperature is below the freezing point of water, the droplets may remain in the liquid state. Such supercooled droplets freeze immediately upon impact with objects in the airflow. This process is usually called accretion. When the temperature of the flux of water droplets towards the object is below the freezing point of water, and each droplet freezes before the next droplet impinges on the same spot, the ice growth is said to be dry. When the water flux increases, the ice growth will tend to be wet, because the droplets do not have the necessary time to freeze, before the next one impinges.

Atmospheric icing of structures, trees, power line cables, road surface, etc. has been the subject of several physical and engineering studies for decades, specially focusing on learning about the accretion process in order to reduce problems and economical loss caused by this phenomenon.

Numerous numerical models have been developed with the purpose of understanding and determining the ice accretion process as well as the structure and morphology of the accreted ice on collectors of different geometries [1–3]. Usually, numerical models require empirical adjustment of parameters such as ice density, temperature of the accretion and heat and mass transfer coefficients [4–7].

The physical properties and the appearance of the accreted ice will vary widely according to meteorological conditions during ice growth. Basically, they depend on the shape and size of the collector (a), the wind speed (V), the air temperature (T), the collector temperature (T_s), the liquid water content (LWC), the droplet size distribution, and the accreted ice density (ρ). Some of these variables are measured directly in the experiments while others need to be determined indirectly by means of other parameters.

The temperature of the collector can be significantly increased by the releasing of the latent heat of fusion as the supercooled water droplets freeze on its surface. This temperature is one of the most important variables involved in the accretion process because it controls the density of the accretion and in consequence it affects the surface characteristics and the appearance that accreted ice achieves. The temperature of the accreted ice is determined by the balance between the rate at which latent heat is released by the freezing of collected water drops and the rate at which heat can be lost by convection and sublimation, i.e. the heat and mass transfer process plays an essential role in the temperature of the accretion. To calculate this temperature it is necessary to introduce parameterizations of the Nusselt number (Nu) and the Sherwood number (Sh), which are dimensionless numbers related to the heat and mass transfer coefficients, respectively [8].

There is experimental evidence [5,7,9,10,15] that the roughness of the accretion affects the air flux in its vicinity and therefore the heat transfer process (Nu). Therefore, the following questions are in order: (1) How are these rough surfaces generated? (2) How is the mass transfer between the accretion and the surroundings when the surface of the sublimating ice is not smooth but rough? In order to provide information regarding these questions, the present work presents studies of ice accretions, together with measurements of their sublimation rate, i.e. mass sublimating from the deposit per unit time. This work also focuses on the structural characteristics of the growing surface. The results presented correspond to three different air-flux velocities for the accretion growth.

* Corresponding author.
E-mail address: avila@famaf.unc.edu.ar (E.E. Ávila).

0017-9310/$ - see front matter © 2009 Elsevier Ltd. All rights reserved.
doi:10.1016/j.ijheatmasstransfer.2009.05.002

Nomenclature

a_{max}	diameter of the ice-covered cylinder (mm)
d_m	median diameter of the spectra of cloud droplet (μm)
Dm	mean diameter of the lobes (mm)
Ew	effective liquid water content (g m^{-3})
K	Stokes' number
L	length of the ice-covered cylinder (mm)
MAR	mass accretion rate (g s^{-1} m^{-2})
t	total time of the accretion process (min)
T	air temperature (°C)
T_s	accretion surface temperature (°C)
V	wind speed (m s^{-1})
V_e	impact velocity at the stagnation point of the cylinder (m s^{-1})
X	Macklińs parameter (μm m s^{-1}°C^{-1})
Greeks	
α	sublimation rate (g s^{-1} m^{-2})
η	surface lobe density (mm^{-2})
η_a	dynamic viscosity of air (kg m^{-1} s^{-1})
ρ	accreted ice density (g cm^{-3})
ρ_a	air density (g cm^{-3})
ρ_w	water density (g cm^{-3})

2. Experimental setup

Ice structures were formed over a cylindrical collector placed inside a cold chamber of height 3 m and floor area 2×3 m^2 and of controlled temperatures ranging from 0 to –30 °C. A vertical upward-flux wind tunnel was mounted inside the chamber. Fig. 1 shows a schematic diagram of the wind tunnel and other devices used in the experiments. A cylindrical rod of diameter $a = 4$ mm was placed in the wind tunnel and connected to a controlled frequency rotation device which allows the rod rotates around its axis (0.5 Hz was used in this study). This device allows the whole cylindrical rod to be accreted and azimuthally symmetric ice deposits were obtained.

The cylinder was placed with its axis orthogonal to the air flowing in the tunnel. A water drop generator was placed at the entrance of the tunnel, which provided the cloud of water drops necessary to produce accretion on the cylinder. The speed of the airflow past the collector (V) was controlled by adjusting the power to an air pump and was determined by using a Pitot-tube type anemometer. The measurements were conducted for air velocities of 5, 8 and 11 m s^{-1} determined with an error of ±0.5 m s^{-1}.

The water droplet sizes were obtained by taking cloud samples with a microscope glass-slide covered with a thin film of 5% formvar solution. Several cloud samples were taken at the position of the collector for different velocities. The samples were analyzed under a microscope, and the droplet sizes were determined. The median diameter (d_m) of the spectra determined was 30, 31 and 30 μm, for $V = 5$, 8 and 11 m/s, respectively. The range of sizes reached 80 μm, and in some cases, drops were found with sizes as large as 100 μm. Fig. 2 is an example of a typical size-distribution histogram, obtained for an experiment corresponding to 5 m/s.

Besides d_m, clouds were also characterized by the effective liquid water content, Ew. This variable represents the amount of liquid water, per unit air volume, which can be collected by the target, $Ew = M/AVt$, where M is the mass of water deposited, A is the effective cross-section in the air flux, V is the air-flux velocity and t is the accretion time. The effective liquid water content

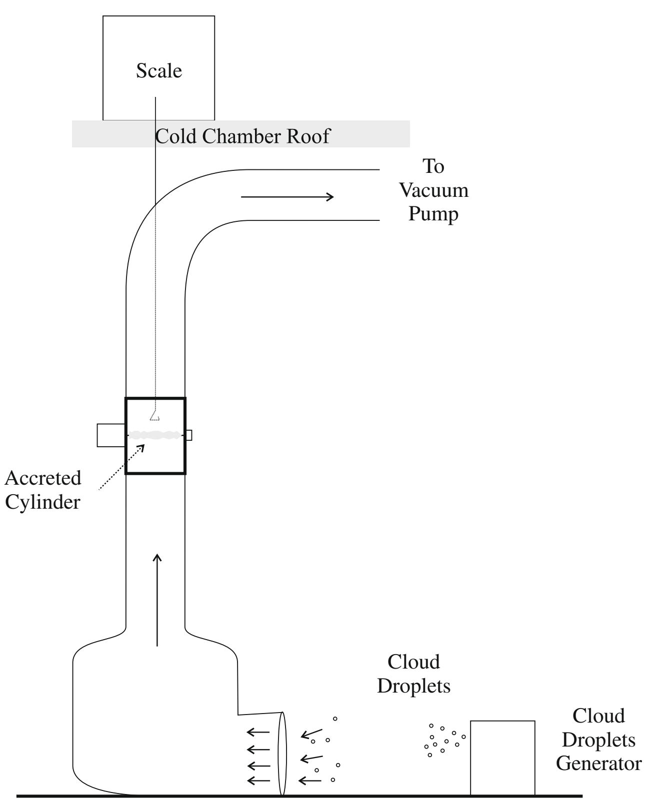

Fig. 1. Sketch of the experimental device used for the laboratory study.

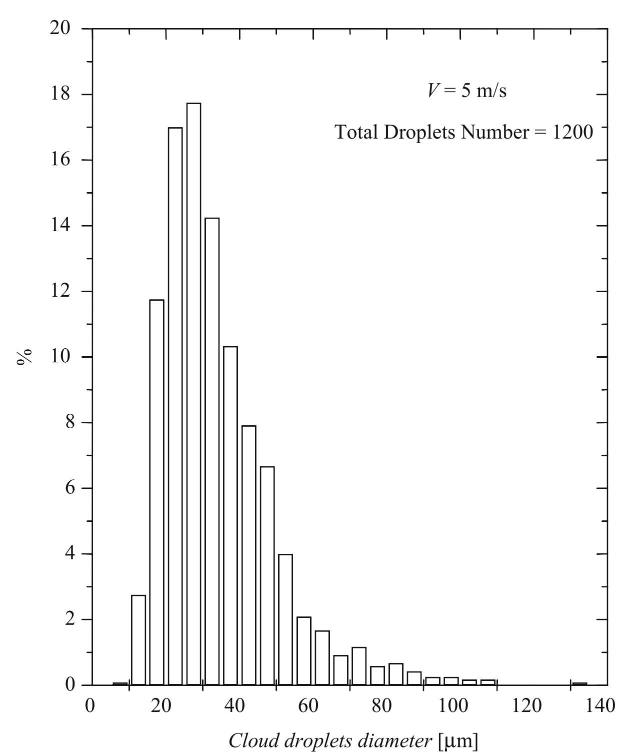

Fig. 2. Cloud droplets size distribution used in the experiments.